

## Geologic mapping of ejecta deposits in Oppia Quadrangle, Asteroid (4) Vesta



W. Brent Garry<sup>a,\*</sup>, David A. Williams<sup>b</sup>, R. Aileen Yingst<sup>c</sup>, Scott C. Mest<sup>c</sup>, Debra L. Buczkowski<sup>d</sup>, Federico Tosi<sup>e</sup>, Michael Schäfer<sup>f</sup>, Lucille Le Corre<sup>c,f</sup>, Vishnu Reddy<sup>c,f</sup>, Ralf Jaumann<sup>g</sup>, Carle M. Pieters<sup>h</sup>, Christopher T. Russell<sup>i</sup>, Carol A. Raymond<sup>j</sup>, the Dawn Science Team

<sup>a</sup> Planetary Geodynamics Laboratory, NASA Goddard Space Flight Center, Greenbelt, MD 20771, USA

<sup>b</sup> School of Earth & Space Exploration, Arizona State University, Tempe, AZ 85287, USA

<sup>c</sup> Planetary Science Institute, 1700 East Fort Lowell, Suite 106, Tucson, AZ 85719, USA

<sup>d</sup> Johns Hopkins University Applied Physics Laboratory, Laurel, MD 20723, USA

<sup>e</sup> Institute for Space Astrophysics and Planetology, Via del Fosso del Cavaliere 100, I-00133 Rome, Italy<sup>1</sup>

<sup>f</sup> Max-Planck-Institute for Solar System Research, Justus-von-Liebig-Weg 3, 37077 Göttingen, Germany

<sup>g</sup> DLR, Berlin, Germany

<sup>h</sup> Department of Geological Sciences, Brown University, Providence, RI 02912, USA

<sup>i</sup> Institute of Geophysics and Planetary Physics, University of California Los Angeles, Los Angeles, CA 90095, USA

<sup>j</sup> Jet Propulsion Laboratory, California Institute of Technology, Pasadena, CA 91109, USA

### ARTICLE INFO

#### Article history:

Received 19 March 2014

Revised 27 July 2014

Accepted 4 August 2014

Available online 8 October 2014

#### Keywords:

Asteroid Vesta

Asteroids, surfaces

Geological processes

Cratering

### ABSTRACT

Oppia Quadrangle Av-10 (288–360°E, ±22°) is a junction of key geologic features that preserve a rough history of Asteroid (4) Vesta and serves as a case study of using geologic mapping to define a relative geologic timescale. Clear filter images, stereo-derived topography, slope maps, and multispectral color-ratio images from the Framing Camera on NASA's Dawn spacecraft served as basemaps to create a geologic map and investigate the spatial and temporal relationships of the local stratigraphy. Geologic mapping reveals the oldest map unit within Av-10 is the cratered highlands terrain which possibly represents original crustal material on Vesta that was then excavated by one or more impacts to form the basin Feralia Planitia. Saturnalia Fossae and Divalia Fossae ridge and trough terrains intersect the wall of Feralia Planitia indicating that this impact basin is older than both the Veneneia and Rheasilvia impact structures, representing Pre-Veneneian crustal material. Two of the youngest geologic features in Av-10 are Lepida (~45 km diameter) and Oppia (~40 km diameter) impact craters that formed on the northern and southern wall of Feralia Planitia and each cross-cuts a trough terrain. The ejecta blanket of Oppia is mapped as 'dark mantle' material because it appears dark orange in the Framing Camera 'Clementine-type' color-ratio image and has a diffuse, gradational contact distributed to the south across the rim of Rheasilvia. Mapping of surface material that appears light orange in color in the Framing Camera 'Clementine-type' color-ratio image as 'light mantle material' supports previous interpretations of an impact ejecta origin. Some light mantle deposits are easily traced to nearby source craters, but other deposits may represent distal ejecta deposits (emplaced >5 crater radii away) in a microgravity environment.

Published by Elsevier Inc. This is an open access article under the CC BY-NC-ND license (<http://creativecommons.org/licenses/by-nc-nd/3.0/>).

### 1. Introduction

Distal ejecta are defined as impact material deposited more than five crater radii away from an impact crater. Examples of

distal ejecta have been identified on Earth (e.g., Chicxulub impact crater) (Pope et al., 2005) and the Moon (Robinson et al., 2011), but have yet to be identified on smaller planetary bodies like asteroids. NASA's Dawn mission to Vesta has provided unprecedented views of the second largest object in the main asteroid belt (Russell and Raymond, 2011; Russell et al., 2012). The surface of Vesta preserves a turbulent history including two large impact basins and a variety of surface materials (Buczkowski et al., 2012; Jaumann et al., 2012; Marchi et al., 2012; Le Corre et al., 2013) providing a challenge to piece together the geologic

\* Corresponding author at: Planetary Geodynamics Laboratory, Code 698, NASA Goddard Space Flight Center, Greenbelt, MD 20771, USA.

E-mail address: [brent.garry@nasa.gov](mailto:brent.garry@nasa.gov) (W.B. Garry).

<sup>1</sup> Address: Istituto di Astrofisica e Planetologia Spaziali, Istituto Nazionale di Astrofisica, Rome, Italy.

evolution of this large asteroid. Here, we use geologic mapping to evaluate if surface units discussed in Reddy et al. (2012) and Le Corre et al. (2013) are distal ejecta deposits on Vesta. Relating these deposits to impact craters several crater radii away will provide new insights into the dynamics of distributing impact crater materials on planetary bodies with low-gravity environments.

Asteroid (4) Vesta is the second largest object in the main asteroid belt ( $286.3 \text{ km} \times 278.6 \text{ km} \times 223.2 \text{ km}$  ( $\pm 0.1 \text{ km}$ ), a mean radius of  $262.7 \pm 0.1 \text{ km}$ ), next to Ceres (e.g., Russell et al., 2004; Rayman et al., 2006; Russell and Raymond, 2011). Based on studies of the Howardite–Eucrite–Diogenite (HED) clan of meteorites, Vesta is a differentiated body (e.g., McCord et al., 1970; McSween et al., 2013). Basaltic compositions imply that there was once volcanic activity on the surface (Wilson and Keil, 1996), but evidence of volcanic activity is not apparent on the surface (Yingst et al., 2014, in press) except in a few potential locations where anomalous topographic mounds are present (e.g., Brumalia Tholus in Av-9) (e.g., Buczkowski et al., 2014). The topography of Vesta varies in elevation between  $-22.3$  and  $19.1 \text{ km}$  (reference ellipsoid  $285 \text{ km} \times 229 \text{ km}$ ) (Jaumann et al., 2012). The total topographic relief on Vesta is  $41.4 \text{ km}$ . The extreme topographic highs and lows create local slopes up to  $40^\circ$  that directly influence the shape of impact craters (Krohn et al., 2013). The geographic south pole of Vesta is dominated by the Rheasilvia impact structure and a central mound, which partially overlaps another large impact basin, Veneneia (Schenk et al., 2012; Yingst et al., 2014, in press, see Fig. 4 in Williams et al., 2014a). One set of troughs wraps around the equatorial belt and a second set through the northern hemisphere; these structures are interpreted to be related to the Rheasilvia and Veneneia impacts, respectively (Jaumann et al., 2012; Buczkowski et al., 2012; Schäfer et al., 2014 (Av-6,7)).

Global mapping of Vesta at 1:500,000 map-scale was completed during the first year using the High-Altitude Mapping Orbit (HAMO) imagery ( $\sim 60 \text{ m/pixel}$ ) from Dawn's cameras (Yingst et al., 2014, in press). The global geologic map of Vesta defined the major rock units on the surface including the Rheasilvia Formation (southern impact), Divalia Fossae Formation (equatorial

trough system), Saturnalia Fossae Formation (northern trough system), heavily-cratered highlands and plains, as well as distinctive surface units – dark and bright crater materials, and a dark mantle (anomalous ejecta) (Yingst et al., 2014, in press). Defining and characterizing the geologic map units is difficult (Williams et al., 2014a), even with the in derived from the Howardite–Eucrite–Diogenite (HED) samples and two different interpretations for crater model-age dating on Vesta (Schenk et al., 2012; Marchi et al., 2012, 2014; O'Brien et al., 2014; Schmedemann et al., 2014). A fundamental approach to defining the geologic history of Vesta is to use geologic mapping to establish a relative stratigraphy of the surface and relative timescale of events (Wilhelms, 1990; Williams et al., 2014a). Systematic mapping of the 15 established quadrangles on Vesta have been used to address a variety of scientific questions (Williams et al., 2014a). Here, we will focus on how a relative geologic timescale can be established through geologic mapping of vestan quadrangle Av-10 (Fig. 1) (Williams et al., 2014b) and the nature of anomalous ejecta deposits (light and dark mantle materials) (Le Corre et al., 2013). With respect to the geology of quadrangle Av-10, we utilize geologic mapping to address the following questions: What is the relative stratigraphy of geologic units and structures in Av-10? What is the geologic context of light and dark mantle material observed in color ratio imagery? Quadrangle Av-10 provides a snapshot of the geologic history of Vesta and an optimal location to discuss the context of light and dark mantle material and a preliminary geologic timescale for the asteroid.

## 2. Data and mapping methods

The introductory paper for this special issue on the geologic mapping of Vesta provides details about the Dawn mission, instruments, data sets, and geologic mapping methods (Williams et al., 2014a) in addition to the overview presented here. NASA's Dawn spacecraft (Russell and Raymond, 2011) documented the surface of Vesta for nearly 14 months (July 16, 2011–September 5, 2012)

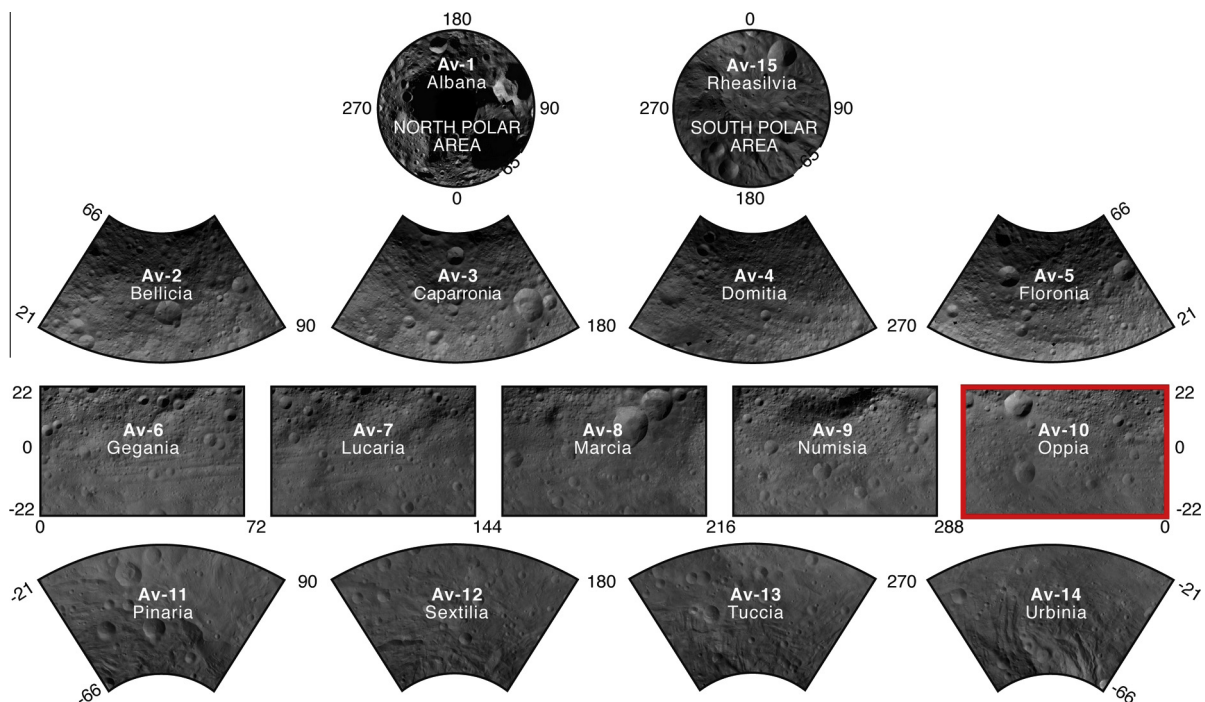
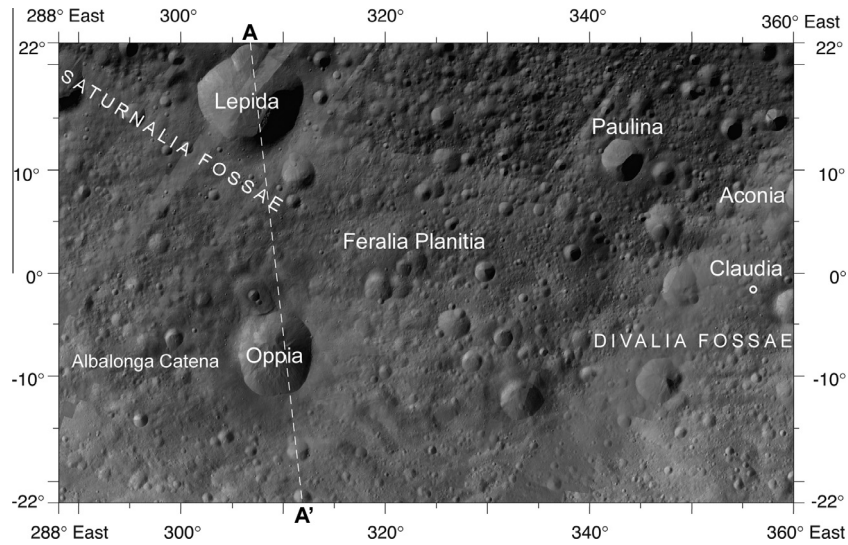
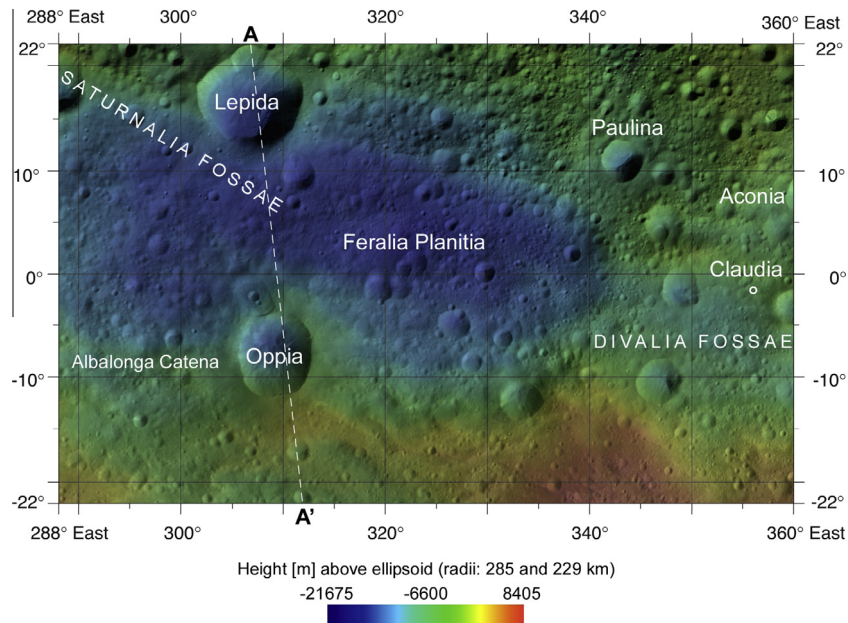


Fig. 1. Layout of the 15 quadrangles for (4) Vesta. Oppia Quadrangle, Av-10, is one of five equatorial quadrangles between  $288^\circ\text{E}$  and  $360^\circ\text{E}$ .



**Fig. 2.** Oppia Quadrangle Av-10: Dawn FC clear filter LAMO mosaic. Dashed white line marks the line of section for the topographic profile in Fig. 9.



**Fig. 3.** Oppia Quadrangle Av-10: topography based on HAMO/HAMO 2 Digital Terrain Model. Dashed white line marks the line of section for the topographic profile in Fig. 9.

with three primary science instruments: the Framing Camera (FC) (Sierks et al., 2011), a visible and infrared spectrometer (VIR) (De Sanctis et al., 2011), and the Gamma Ray and Neutron Detector (GRaND) (Prettyman et al., 2011, 2012). Data collection was subdivided into four main orbital campaigns: Survey (2700 km, 252 m/pixel), High-Altitude Mapping Orbit (HAMO) (660–730 km, 61 m/pixel), Low-Altitude Mapping Orbit (LAMO) (190–240 km, 16 m/pixel) and a second High-Altitude Mapping Orbit (HAMO-2) (640–730 km, 60 m/pixel) prior to departure. The FC (Sierks et al., 2011) has a clear filter and 7 narrow-band filters (0.4–1.0  $\mu\text{m}$ ) that mapped near global coverage of the surface. The image resolution ranged between 16 and 487 m/pixel based on the different altitudes over mean surface. Color filter data were used to create a false color-ratio mosaic using ratios comparable to the ones used by NASA's Clementine mission to explore the Moon (red: 750/430 nm, green: 750/920 nm, blue: 430/750 nm) (Pieters et al., 1994; Le Corre et al., 2011; Reddy et al., 2012). A 'true color' image was also produced using the following FC color filters (red chan-

nel = filter #7 (650 nm), green channel = filter #2 (550 nm), blue channel = filter #8 (430 nm)). The VIR instrument (De Sanctis et al., 2011) is an imaging spectrometer in the overall spectral range from 0.25 to 5.1  $\mu\text{m}$ , capable to determine the mineral composition of surface materials in their geologic context, and to derive spatially-resolved thermal maps of the asteroid on its dayside and above  $\sim 180$  K (Tosi et al., 2014). GRaND collected data mostly during LAMO and measured the elemental composition of the regolith. Initial results of the global survey of near infrared spectra, as well as Fe/O and Fe/Si ratios, show that the surface is consistent with howardite-like regolith containing varying proportions of eucrite and diogenite at different locations (De Sanctis et al., 2012; Prettyman et al., 2012). A Digital Terrain Model and corresponding slope map have been derived from FC clear filter stereo-images (Gaskell, 2012).

Geologic mapping was completed in ArcGIS 10.2 using a set of georeferenced mosaics and DTMs provided by the Dawn Science Team. We present the full resolution geologic map at a 1:250,000

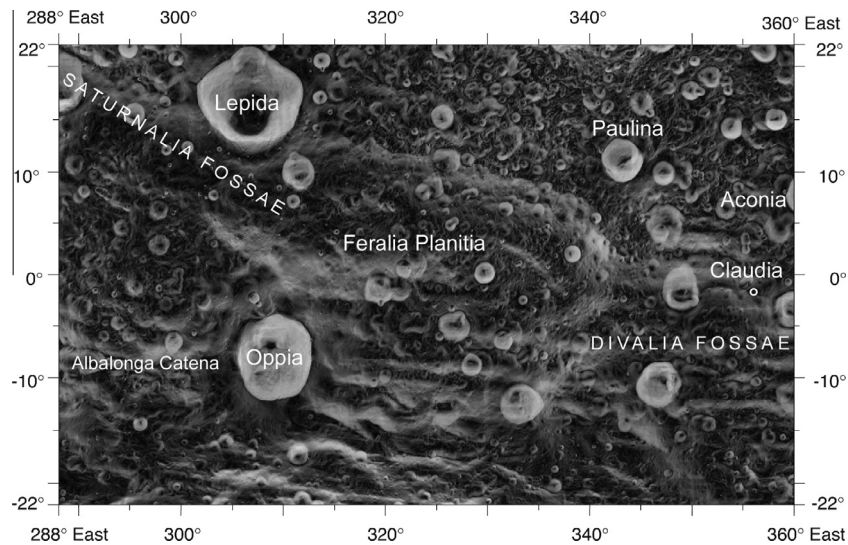


**Fig. 4.** Oppia Quadrangle Av-10: slope map based on HAMO/HAMO 2 Digital Terrain Model.

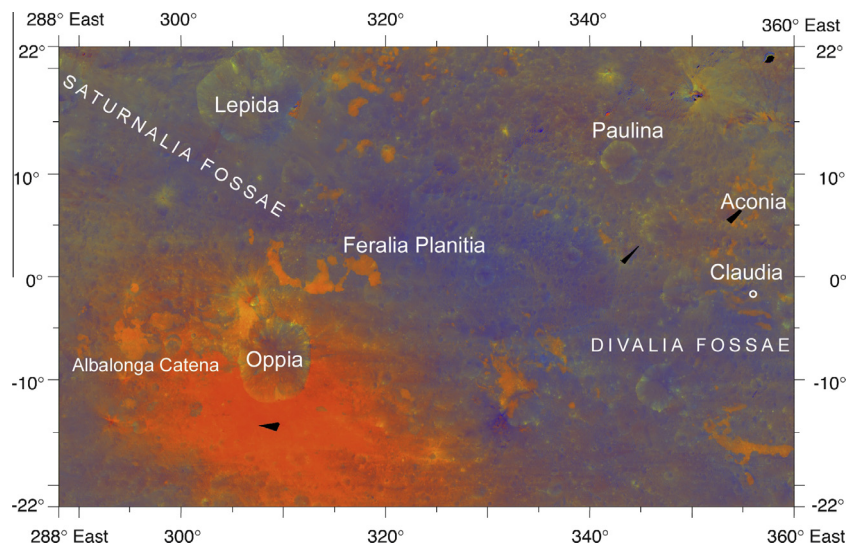


**Fig. 5.** Oppia Quadrangle Av-10: 'Clementine' color-ratio image [red (750/430 nm), green (750/920 nm), blue (430/750 nm)]. (For interpretation of the references to color in this figure legend, the reader is referred to the web version of this article.)

map scale ([supplemental material](#)); latitude–longitude are given in the Dawn Claudia coordinate system (Russell et al., 2012; Roatsch et al., 2012; Williams et al., 2014a), rather than the Planetary Data System (PDS) coordinate system (Claudia coordinate system = [PDS 2013 longitude] – 150°). The primary basemap used for mapping physical geologic units was FC LAMO clear filter mosaic with data gaps filled in by HAMO imagery (Fig. 2). Topographic profiles and measurements of feature dimensions were obtained from the Gaskell HAMO-2 shape model of Vesta (Fig. 3) and associated slope map (Fig. 4), extracted in the software analysis program, JVesta, which is publicly available at <http://jmars.asu.edu> (Christensen et al., 2009). The FC color-ratio mosaic (Fig. 5) and 'true color' image (Fig. 6) were used to map surface materials with distinctive multispectral properties, not apparent in the clear filter mosaic.

### 3. Geologic setting and features of Oppia Quadrangle Av-10

Oppia Quadrangle Av-10 is one of five equatorial quadrangles on Vesta that covers the area 288–360°E and 22°S to 22°N (Figs. 2–6). The central area of Av-10 is dominated by a broad, east–west

elongated basin (Ferialia Planitia). This basin is surrounded by topographically higher cratered terrain in the northeast quadrant and a relatively smoother, faulted terrain along the southern border. Structural troughs strike through Av-10 from the northwest (Saturnalia Fossae) and the southeast (Divalia Fossae) corners. The two largest craters in Av-10 (Oppia, Lepida), both >35 km in diameter, are located along the perimeter of Ferialia Planitia. Some of these geologic features extend into adjacent quadrangles where their morphologic characteristics are better represented (Fig. 7). To the west, is Numisia quadrangle Av-9, which is dominated by ancient cratered highland feature, Vestalia Terra (Buczkowski et al., 2014). To the east are Gegania quadrangle Av-6 and Lucaria quadrangle Av-7, where troughs in the Divalia Fossae Formation are best preserved (Schäfer et al., 2014). To the north is Floronia quadrangle Av-5 (Ruesch et al., 2014; Scully et al., 2014) dominated by cratered highlands and Saturnalia Fossae Formation. To the south is Urbinia quadrangle Av-14, which is dominated by the Rheasilvia impact structure (Rheasilvia quadrangle Av-15) (see Fig. 4 in Williams et al., 2014a). Here, we discuss the characteristics of geologic features formally named by the International Astronomical

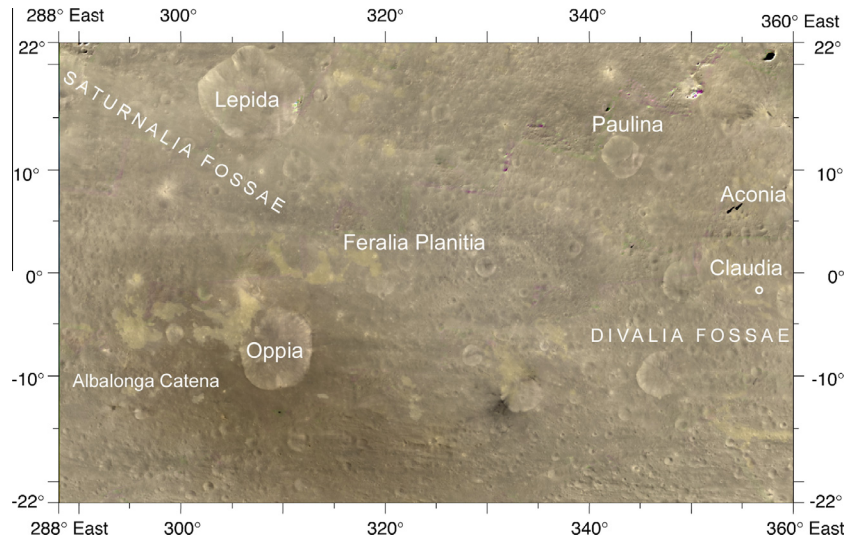


**Fig. 6.** Oppia Quadrangle Av-10: ‘true color’ image [red channel = filter #7 (650 nm), green channel = filter #2 (550 nm), blue channel = filter #8 (430 nm)]. (For interpretation of the references to color in this figure legend, the reader is referred to the web version of this article.)

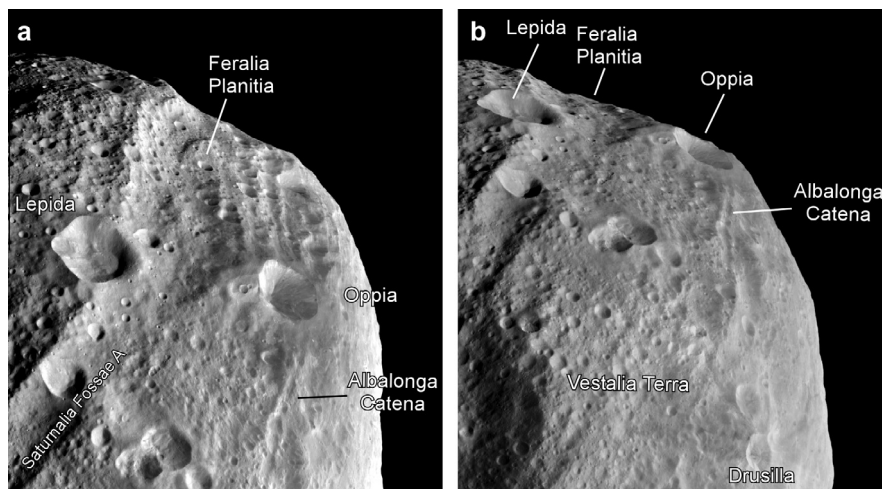


**Fig. 7.** Regional perspective views of the area covered by geologic quadrangle Av-10. Look direction is to the east. The images are from Dawn’s Survey orbit (cycle 6): (a) FC image: FC21B0006400\_11238081914F1A, 254 m/pixel, incidence angle: 37°. (b) FC image: FC21B0006405\_11238084414F1A, 254 m/pixel, incidence angle: 36° [NASA/JPL/DLR].

Union (IAU) followed by a description of mapping units defined in the geologic map in Av-10.

### 3.1. Geologic features

*Oppia crater*, 35–40-km diameter and centered at 309°E, 8°S, is the second largest crater in Av-10 (Fig. 8). Oppia has a sharp rim along the majority of the crater rim, but it is rounded along the northwest (downslope side) (Fig. 8a). Oppia has an asymmetric topographic profile (Fig. 9). The northern half of the rim is at a lower elevation (~27,000 m) than the southern rim (~31,600 m) and the crater floor is at an elevation of ~18,600 m (crater depth = ~8000 to 13,000 m). No outcrops, layers, or boulders are observed within the interior crater wall, but lobes of mass wasting material are present (Fig. 8a). Slopes are 20–30° (southern interior wall) and 30–40° (northern interior wall). Oppia cross-cuts the Divalia Fossae equatorial trough system (Fig. 2) and the shape of the eastern rim is recessed where it intersects ridges and protrudes where it encounters troughs (Figs. 3 and 4).

Crater size frequency distribution measurements on Oppia’s ejecta blanket yield a crater model age of  $276 \pm 23$  Ma (lunar derived chronology: Le Corre et al., 2013). Oppia’s continuous ejecta blanket has an ellipsoidal shape, an asymmetric distribution, and a gradational boundary. Ejecta are primarily distributed to the south, up to 120 km, across the rim of the Rheasilvia impact structure. The ejecta blanket is smoothest and relatively uncratered up to 20 km away from the rim (Fig. 8a) (Le Corre et al., 2013). In FC clear filter images, Oppia’s ejecta blanket does not display any bright or dark crater rays or streaks (Jaumann et al., 2012; Yingst et al., 2014 (in press)). However, the continuous ejecta blanket does have a noticeably darker tone than some of the adjacent craters and surface material (Fig. 8a and d). When viewed in the FC ‘Clementine-type’ color-ratio image, the ejecta blanket of Oppia appears as a dark orange color, distinct from the surrounding purple, blue, and green colors (Figs. 3 and 8c) (Le Corre et al., 2013). The dark orange false-color is most intense near the rim of Oppia and less intense (more diffuse) with increasing distance from the crater center. To the west and northwest of Oppia, the dark orange

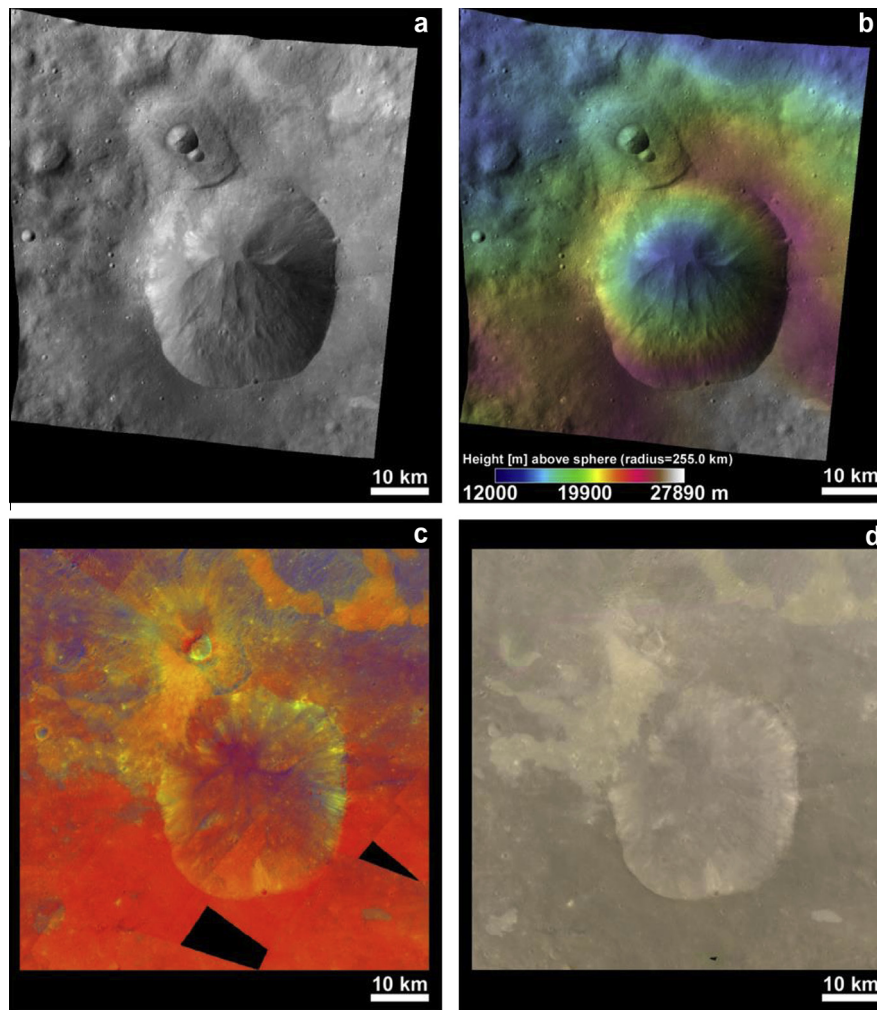


**Fig. 8.** Oppia crater, 35–40-km diameter and centered at 309°E, 8°S: (a) FC HAMO cycle 3 image FC21B0009982\_11284200737F1A, incidence angle: 42°, resolution: 65 m/pixel, (b) topography, (c) ‘Clementine’ color-ratio and (d) “true color” mosaic. (For interpretation of the references to color in this figure legend, the reader is referred to the web version of this article.)

mantle material is discontinuous, interspersed with patches of ‘light orange’ mantle material (Figs. 5 and 8c, d). It is difficult to determine which dark and light orange units in the color-ratio image are associated with Oppia and which deposits are related to other craters due to the overlap, mixing, and degradation of the deposits.

On the northwest rim of Oppia are a relatively fresh, ~5 km diameter crater and ~3 km diameter crater formed on what appears to be a ~10 km diameter crater still preserved on the north sloping face (Fig. 8a and b). We cannot determine if material along Oppia’s rim northwest rim, that appears as a light orange swath in the color-ratio image (Fig. 8c), originated from the 5-km or 10-km diameter crater or Oppia. Of note, the downslope, interior wall on the 5 km crater has a dark orange coloration in the color-ratio image similar to Oppia’s ejecta blanket.

*Lepida crater*, the largest crater in quadrangle Av-10, is 45–48-km in diameter and centered at 306.8°E, 16.7°N (Fig. 2). *Lepida* crater is located along the northern wall of Feralia Planitia directly opposite Oppia crater. However, *Lepida*’s ejecta blanket does not exhibit the same dark orange color in FC ‘Clementine-type’ false-color ratio image as Oppia (Fig. 5). The rim of *Lepida* is sharp around the northern rim and rounded on the southern (downslope) side, and contains kinks along the eastern and western sections of the rim where it intersects Saturnalia Fossae A. The crater wall is relatively featureless except for a few lobes related to mass wast-

ing, with no outcrops or boulders present. *Lepida* has an asymmetric topographic profile similar to Oppia (north rim: 19,800 m, south rim: 16,900 m, depth: ~5000 to 8000 m), but the floor is relatively flat compared to Oppia’s floor (Fig. 9). The continuous ejecta blanket is distributed roughly symmetrical around the crater onto the floor of Feralia Planitia, across the Saturnalia Fossa A trough, and onto the cratered highlands in the northeast. No dark or bright crater-ray material is associated with *Lepida*’s ejecta blanket. In the color ratio image, patches of light orange appear to northeast of the crater rim, but it is unclear if any originated from the *Lepida* impact event.

*Paulina crateris* 19-km in diameter and centered at 343.1°E, 11°N (Fig. 2). This crater is located within the more densely cratered area in the northeast quadrant of Av-10. *Paulina* has a more symmetrical topographic profile than Oppia and *Lepida*. The crater rim is at an elevation of 24,500–26,000 m, with a depth of 4000–5000 m. The ejecta blanket is smoothest up to ~8 km away from the rim. No dark or bright ejecta material is associated with this crater.

*Claudia crater* is a 0.65–0.7 km diameter crater centered at 356°E, 1.65°S. *Claudia* crater has the distinction of being chosen as the benchmark crater to establish the 356°E longitude line and define the *Claudia* coordinate system currently used by the Dawn team (Fig. 10) (Russell et al., 2012; Roatsch et al., 2012; Williams et al., 2014a). The crater is located at an elevation of

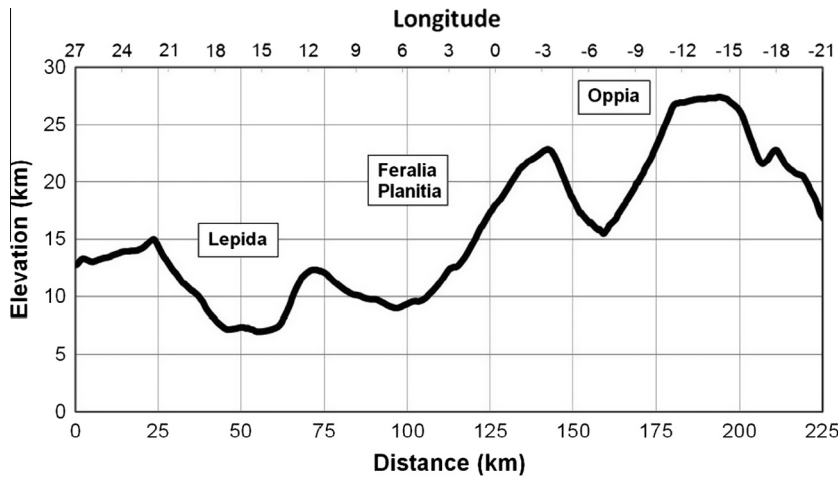


Fig. 9. Topographic cross-section across Lepida, Ferialia Planitia, and Oppia. Elevation data extracted from the HAMO 1-2 Digital Terrain Model (DLR 2013-05-24) in JVesta.

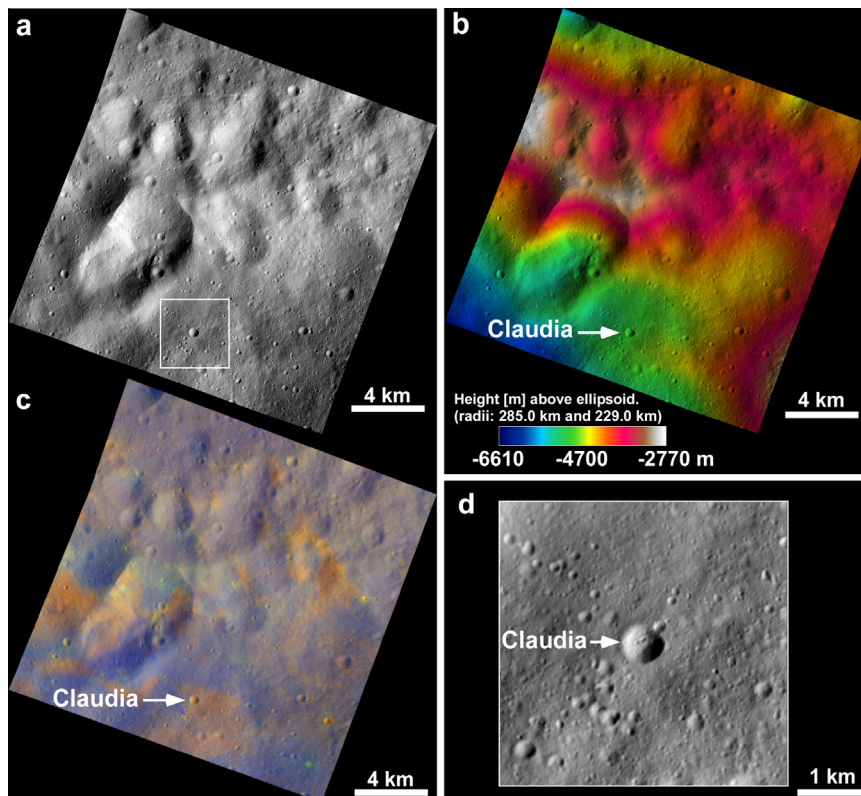


Fig. 10. Claudia crater is a  $\sim 0.65\text{--}0.7$  km diameter crater, centered at  $356^\circ\text{E}$ ,  $1.65^\circ\text{S}$ , that is the control point that defines the  $356^\circ$  longitude line for the Claudia coordinate system used in the geologic maps in this special issue (Williams et al., 2014a). (a) Framing Camera LAMO image, (b) topography, (c) clementine color-ratio, and (d) subset detail of Claudia. (For interpretation of the references to color in this figure legend, the reader is referred to the web version of this article.)

$\sim 29,750$  m and straddles a terrain boundary between cratered highlands terrain and Divalia Fossae Formation. The crater is symmetrical, but the western rim appears slightly rounded compared to the sharper eastern rim. Claudia crater appears to have formed in the ejecta blanket of an unnamed crater, 17-km in diameter, centered at  $0^\circ$ ,  $3.5^\circ\text{S}$ . Claudia is also located within a patch of material that appears light orange in the color ratio image, but Claudia does not appear to excavate this unit (Fig. 10c).

*Ferialia Planitia* is a topographic basin that is bound to the west by Vestalia Terra (Av-9) (De Sanctis et al., 2014; Buczkowski et al.,

2014), the rim of Rheasilvia to the south (Av-14) (Williams et al., 2014a), Divalia Fossae troughs (Av-6) to the east and cratered highland terrain (Av-5) to the northeast (Ruesch et al., 2014; Schäfer et al., 2014; Scully et al., 2014) (Figs. 2 and 3). The basin has an ellipsoidal shape (120–130 km by 300 km) with the long axis in the east–west direction ( $288\text{--}343^\circ\text{E}$ ) and minor axis in the north–south direction ( $8.5^\circ\text{S}$  to  $13^\circ\text{N}$ ). The depth of the basin is 5–7 km from the northern rim and up to 14 km along the southern wall near Oppia (Fig. 9). The rim around Ferialia Planitia is degraded by impact craters and the floor is mixture of highly cratered terrain and areas resurfaced by impact ejecta. Troughs from Saturnalia

Fossae and Divalia Fossae Formation intersect the northwest and southeast rim of the basin (Fig. 3).

*Divalia Fossae*, the equatorial ridge and trough system, is present in the southeast quadrant of Av-10 (Fig. 2). A detailed study of this trough system is discussed in the papers on quadrangles Av-6 and Av-7 (Schäfer et al., 2014). At least four troughs can be defined in Av-10 based on topography and slope (Figs. 3 and 4). Collectively, these troughs spread across a north–south span of 50 km visible in the quadrangle from latitude 0 to 13°S. The ridges between the troughs are not sharp and have been degraded by impacts. The troughs can be traced across the eastern rim of Feralia Planitia until they are truncated by the eastern rim of Oppia crater. However, the same set of troughs are not well-defined on the western side of Oppia. Within the confines of Av-10, the troughs are 11–14 km wide and ~1–2 km deep, but have been measured as deep as 5 km in Av-6 (Schäfer et al., 2014).

*Saturnalia Fossa A* is located in the northwest corner of Av-10 (292°E, 16°N) and trends northwest–southeast at ~115° (Fig. 2). This structural feature is part of a series of troughs located in the northern hemisphere on Vesta that are not visible in Av-10. By itself, *Saturnalia Fossae A* is ~365 km long and 40 km wide (Buczkowski et al., 2012; Scully et al., 2014), but only ~60 km is present in Av-10. Within Av-10, the trough is ~40 km wide and 4 km deep, with slopes up to 25°. *Saturnalia Fossae A* intersects the northeastern rim of Feralia Planitia, but is superposed by Lepida crater. The northern ridge/wall is well-defined, but the southern ridge is not apparent on the floor of Feralia Planitia.

Topographic data suggests a subtle expression of *Saturnalia Fossa A* may be present on the floor of Feralia Planitia (Fig. 3). A detailed study of the *Saturnalia Fossae* trough system is presented in Scully et al. (2014).

*Albalonga Catena* is an east–west trending lineation that is ~200 km long, but only 80 km of this feature is present in Av-10 (288–301°E, 8.5°S) (Fig. 2). The eastern end of this feature is truncated and overprinted by Oppia crater. *Albalonga Catena* is characterized by a series of pits with an east–west alignment and is referred to as a pit chain. What is unique about this feature is that it begins as a series of merged pits in the east, but transitions to a topographic high known as *Brumalia Tholus* on *Vestalia Terra* at the western end of the lineament (De Sanctis et al., 2014; Buczkowski et al., 2014). A detailed discussion on the origin of this feature is presented in Buczkowski et al. (2014).

### 3.2. Description of Mapping Units (DOMU)

We have identified 10 different geologic units in Av-10. The units are discussed from apparent oldest to youngest. Type locations of each unit in FC clear filter images are presented in Fig. 11. Geologic units were defined based on characteristics observed in different data sets and mapped on the FC LAMO mosaic. The geologic map, map legend, and correlation of map units (COMU) are presented in Fig. 12. The map is presented at 1:250,000 map scale in the supplemental material.

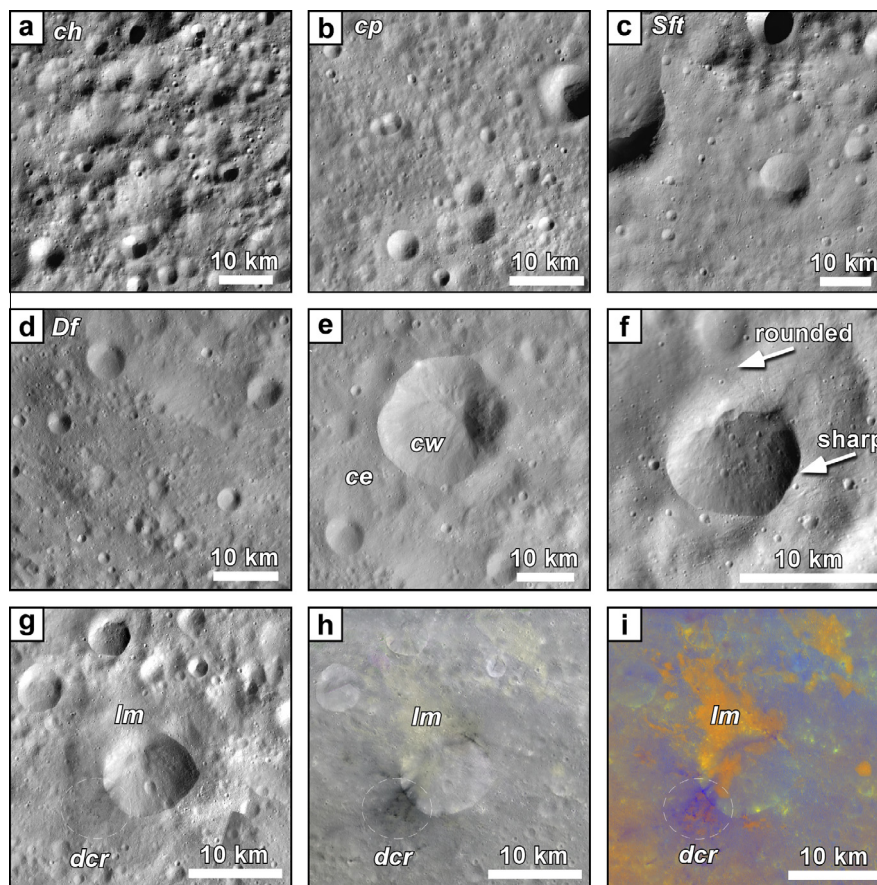


**Fig. 11.** Type locales of the geologic mapping units in Oppia Quadrangle Av-10. Images subsets of the Framing Camera clear filter LAMO global mosaic. (a) Cratered highlands material (9.6–20.0°N, 326.5–337.6°E), (b) cratered plains material (–3.8 to 4.3°N, 330.8–338.7°E), (c) *Saturnalia Fossae* formation (10.8–21.8°N, 288.0–299.7°E), (d) *Divalia Fossae* formation (–22.0 to –12.75°N, 340–350°E), (e) crater wall material and crater ejecta (–16.2 to –6.8°N, 342.15–351.8°E), (f) crater with asymmetric rim – rounded (downslope) and sharp (upslope) (–8.2 to –4.1°N, 329.7–333.6°E). Three views of the same location are shown in (g), (h), and (i) (–5.14 to –17.3°N, 327–339.5°E), (g) dark crater ray material and light mantle (multispectral unit) in Framing Camera clear filter, (h) FC ‘true color’, and (i) FC ‘Clementine’ color-ratio. Rheasilvia Smooth terrain is not shown. Dark mantle multispectral unit is shown in Fig. 8c. Incidence angles for the FC images range from ~30° to 65°.

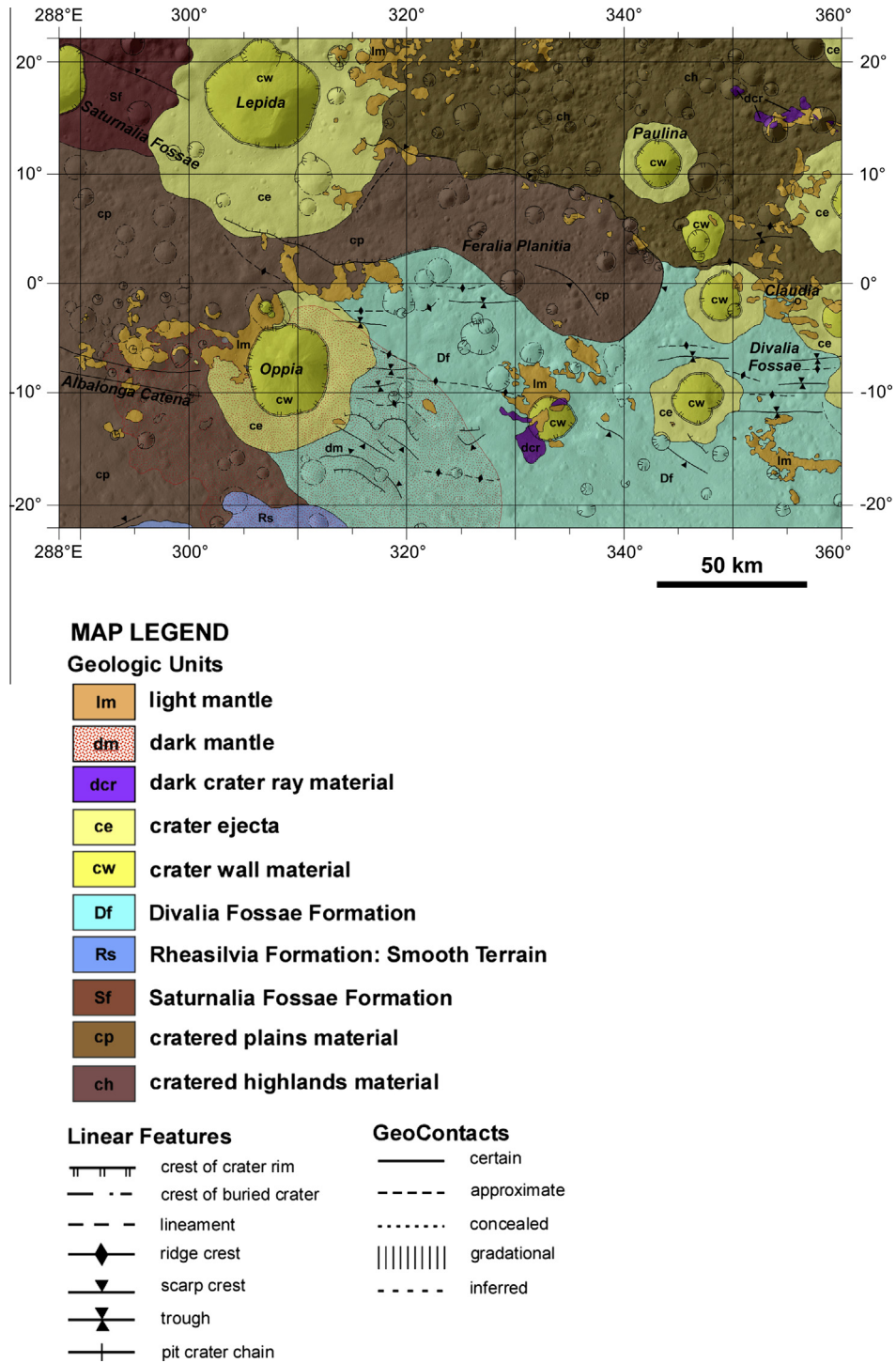


Fig. 12. (a) Geologic map of Vesta quadrangle Av-10 “Oppia” based on Dawn FC LAMO imagery (~20 m resolution), (b) map legend, and (c) correlation of map units (COMU).

3.2.1. Cratered highland terrain (ch)

This unit is defined as the area with the highest concentration of impact craters in Av-10 (Fig. 11a). On the geologic map, this unit is located in the northeastern quadrant of Av-10, confined to the topographically higher area that bounds Ferialia Planitia (Fig. 12). The craters in this area have both degraded and sharp crater rims. Portions of this unit have been resurfaced by ejecta from younger craters including Lepida and Paulina. The unit extends beyond the map boundary of Av-10 to the north and east into quadrangles Av-5 and Av-6. In the FC Clementine-type color-ratio image, this cratered highlands terrain is a mix of blue and purple with green

accents around crater rims (Fig. 5). Interpretation: This unit is interpreted to be the oldest vestan crustal material present in Av-10 based on the high density of degraded craters on a topographically high area. This unit is described on the global geologic map as a heavily cratered terrain and interpreted as an ancient terrain, possibly a Pre-Veneneian remnant of original Vesta crust (Yingst et al., 2014, in press; Williams et al., 2014b).

3.2.2. Cratered plains material (cp)

This unit also has a high concentration of craters (Fig. 11b), but is mapped as a different unit from the cratered highlands (ch) unit

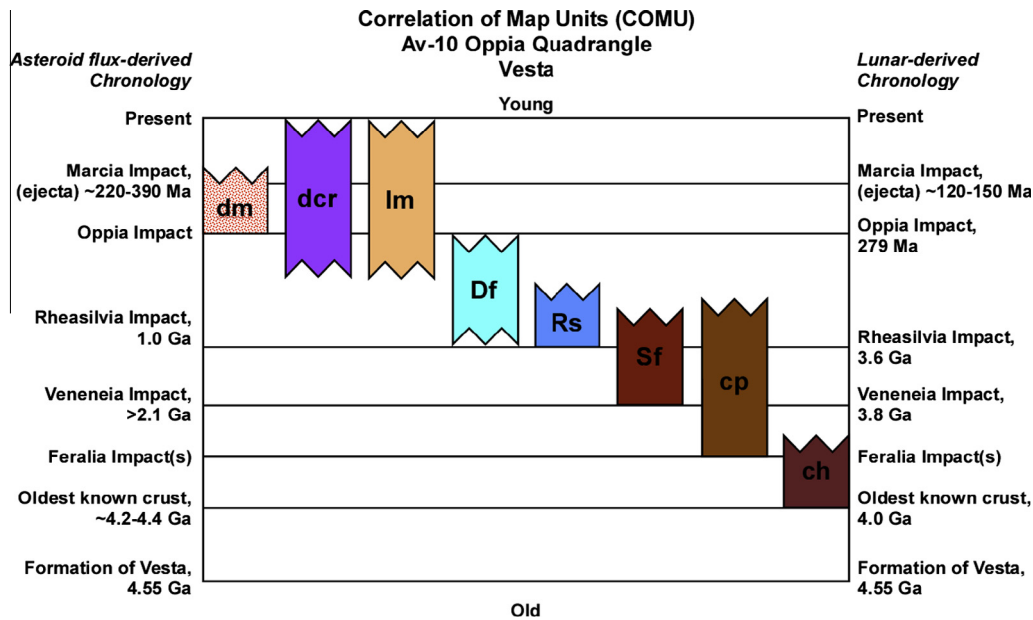


Fig. 12 (continued)

because it is confined to the floor of a topographic basin – Feralia Planitia (Fig. 8). Ejecta from younger craters have obscured parts of this unit. In the FC color-ratio image, the surface material in this unit appears as blues and purples (Fig. 3). *Interpretation:* Within Av-10, this unit represents the degradation of the floor of an ancient basin that formed in the cratered highlands terrain (*ch*). On the global map this unit is interpreted as an ancient cratered terrain that has been modified by ejecta from Rheasilvia and younger impacts (Yingst et al., 2014, in press).

### 3.2.3. Saturnalia Fossae Formation: trough terrain (*Sft*)

The portion of *Saturnalia Fossa A* that is present in the northwest corner of Av-10 has been mapped as the Saturnalia Fossae Formation trough terrain (Fig. 11c). Globally, this unit is characterized by a series of northwest-southeast trending troughs that are prominent in the heavily cratered northern vestan quadrangles (Yingst et al., 2014, in press; Ruesch et al., 2014; Scully et al., 2014). We have mapped this as a different unit from *ch* unit because of the presence of the large trough. *Interpretation:* The troughs are interpreted to be a tectonic response by the crust to the Veneneia impact event (170°E; 52°S) (Buczkowski et al., 2012; Schenk et al., 2012). On the global map this unit is interpreted as ancient crust that has been cut by fault-bounded grabens and degraded over time, representing one of the more ancient terrains on Vesta (Yingst et al., 2014, in press).

### 3.2.4. Rheasilvia Formation: smooth terrain (*Rs*)

A sliver of the Rheasilvia Formation – smooth terrain is mapped along the southern border of Av-10 between 290°E and 310°E (Fig. 12) (see geologic maps of Av-14 and Av-15 in Fig. 4 in Williams et al., 2014a). This unit is defined in Av-10 by material at the base of southward facing scarps related to the Rheasilvia impact structure. This unit is smoother and not as heavily cratered as the *ch*, *cp*, or *Sf* units in Av-10. *Interpretation:* This unit is terrain related to the impact event that formed Rheasilvia, which is geologically younger than Veneneia (Buczkowski et al., 2012; Schenk et al., 2012). The global map interprets this unit as ejecta material related to Rheasilvia (Yingst et al., 2014, in press). Refer to the discussions and geologic maps for Av-11, Av-12, Av-13 for further

characterization and interpretation of this terrain (Kneissl et al., 2014).

### 3.2.5. Divalia Fossae Formation (*Df*)

This unit is defined by a series of troughs and ridges, parallel to the equatorial belt of Vesta (Fig. 11d) that are present between 0–15°S and 310–360°E in the southeastern corner of quadrangle Av-10 (Fig. 12). The troughs are mapped on the eastern side of Oppia crater (340–360°E), and on the floor of Feralia Planitia, but not on the western side of Oppia (Fig. 12). The southern portion of the *Df* terrain in Av-10 is the topographically highest region in the quadrangle and is characterized by north-facing scarps, but no troughs. *Interpretation:* The equatorial troughs are interpreted to be the response by crustal material to the Rheasilvia impact event (Buczkowski et al., 2012; Schenk et al., 2012; Yingst et al., 2014, in press). Global mapping shows that this unit is geologically younger than Veneneia impact event (Buczkowski et al., 2012; Schenk et al., 2012; Yingst et al., 2014, in press).

### 3.2.6. Crater materials: crater wall (*cw*) and crater ejecta (*ce*)

We have mapped the main crater cavities of large (>20 km diameter) impact craters with geologically fresh features (smooth, low crater density) as crater materials (Figs. 11e, f and 12). The interior cavities are mapped as crater wall (*cw*) and associated crater ejecta as (*ce*). The ejecta from several of these craters (e.g., Oppia, Lepida, Paulina) have obscured several units and tectonic features in Av-10. *Interpretation:* These materials are the result of more recent (than Rheasilvia) impacts (<500 Ma?) onto more ancient rock units on Vesta. The ejecta blankets have variable coloration in FC Clementine color-ratio imagery.

### 3.2.7. Dark crater ray material (*dcr*)

This unit is characterized by lower albedo material in FC clear filter mosaic and is typically associated with impact craters. In Av-10, this unit is not very common and is only mapped in two locations (Fig. 12). The best exposure is associated with an unnamed crater (333°E, 13°S), ~120 km east of Oppia crater, located within the Divalia Fossa Formation (Fig. 11g–i). The other exposure is located in the cratered highland terrain at (355°E, 14°N). This is a surficial unit that extends from crater rims or

surrounds smaller impacts on the rims of larger craters. This unit appears as a dark purple color in the FC color-ratio images (Fig. 11h). *Interpretation:* On the global map, this unit is interpreted as ejecta from impacts into a thin, discontinuous surface layer of low-albedo material (Yingst et al., 2014, in press).

### 3.3. Multi-spectral surface units

In addition to the geologic surface units described above, we have mapped the distribution of two multispectral units observed in the FC color-ratio image on the geologic map: the light orange and dark orange materials (Fig. 5). We have singled out the surface materials that appear as orange colors in the color-ratio image because the dark orange color is related to Oppia's ejecta blanket and the light orange unit forms distinct, irregular patches, but has a non-uniform distribution across the surface of Av-10 (Fig. 12).

#### 3.3.1. Multispectral surface unit #1: light mantle (*lm*)

This multispectral unit is defined as surface material that appears as the lighter orange color in the FC color-ratio image (Figs. 5, 8c and 11i). In the true color mosaic, the material appears as a lighter, off white color (Figs. 6, 8d and 11h). These individual patches have irregular shapes and are typically associated with the rims of both fresh and degraded impact craters (Fig. 12). Within Av-10, the light orange unit is concentrated within the topographically higher elevations around Feralia Planitia, with only a few patches located along the southern wall of the basin on the north side of Oppia (Fig. 12). *Interpretation:* Le Corre et al. (2013) have interpreted this material to be associated with impact ejecta and possibly represents a mix of impact melt with ejecta.

#### 3.3.2. Multispectral surface unit #2: dark mantle (*dm*)

The second multispectral unit we have mapped appears as a dark orange color in the FC color-ratio image (Figs. 5 and 8c). This multispectral unit is distributed to the south of Oppia crater and overlies cratered plains material, the Divalia Fossae Formation, and the Rheasilvia Formation: Smooth Terrain (Fig. 12). This is not the only crater on Vesta to exhibit the dark orange color in the color-ratio image. Ejecta blankets surrounding Octavia crater (Av-8) (35-km diameter, 146°E, 3°S) and Arruntia crater (11-km diameter, 71°E, 39.3°N) (Av-2) also exhibit this dark orange color in the FC color ratio image (Le Corre et al., 2013; Ammannito et al., 2013; Williams et al., 2014; Ruesch et al., 2014; Schäfer et al., 2014; Scully et al., 2014). *Interpretation:* This multispectral unit is interpreted to be ejecta from Oppia crater that mantles the surface and has a gradational, diffuse boundary.

## 4. Discussion

### 4.1. Geologic context of dark mantle and light mantle 'orange material' on Vesta

#### 4.1.1. Previous studies and interpretations of dark and light mantle material

Observations of surface materials that appear light and dark orange in the color-ratio image (referred to as light and dark mantle in this discussion) were initially described by Reddy et al. (2012), and were followed up by a more detailed study that investigated the origin of these units by Le Corre et al. (2013). The light and dark mantle units have been classified into three types: (a) diffuse ejecta deposits associated with medium-sized impact craters (dark mantle), (b) well-defined lobate patches (light mantle), and (c) ejecta rays from fresh craters (light and dark mantle) (Le Corre et al., 2013). Globally, light and dark mantle units are con-

centrated in the equatorial region of Vesta and are noticeably absent from Rheasilvia basin. Le Corre et al. (2013) concluded that the patches of light and dark mantle are from impact ejecta and impact melt. However, it is unclear if the unique appearance is related to the bedrock material or due to characteristics from the impactor. Several other possible sources were also considered, but ruled out by Le Corre et al. (2013) including: a cumulate eucrite layer exposed by impacts, remnant material from the impactor, or an olivine-orthopyroxene mixture. Le Corre et al. (2013) suggest the majority of the light mantle patches may be related to the formation of Rheasilvia basin, despite the lack of light mantle patches within the basin itself.

The dark mantle present in Av-10 is associated with the ejecta blanket from Oppia crater. Dark mantle material is not present in smaller patches within the quadrangle, as is typically observed for the light mantle unit. Octavia and Oppia have several similarities (Le Corre et al., 2013; Williams et al., 2014; Schäfer et al., 2014). Octavia has a similar crater diameter (~35 km) and has an ejecta blanket that is relatively evenly distributed with a diffuse, gradational boundary as observed at Oppia (Le Corre et al., 2013; Williams et al., 2014; Schäfer et al., 2014). Additionally, Octavia is located at roughly the same latitude as Oppia, but almost directly on the opposite side of Vesta. Oppia and Octavia both overlap the equatorial troughs and are mapped within the Divalia Fossae Formation on opposite sides of Vestalia Terra. There is a slight elevation difference between the two craters. The elevation of the rim and floor of Oppia are ~7000 to 10,000 m below Octavia, but both are still associated with higher topographic terrains, with Octavia just beyond the rim of Veneneia and Oppia just beyond the rim of Rheasilvia. Arruntia is located in the northern hemisphere, has a smaller crater diameter and its ejecta blanket displays crater rays rather than a diffuse deposit (Ruesch et al., 2014; Scully et al., 2014). There is no clear reason as to why there are only three prominent ejecta blankets that exhibit this dark orange color in the color ratio mosaic. The resulting continuous ejecta blankets of dark mantle unit could be due to unique properties of the bedrock or impactor.

#### 4.1.2. Distribution of light mantle deposits in Av-10

Our mapping supports the initial interpretation by Le Corre et al. (2013) that the light and dark mantle units are related to impact ejecta (melt?). The map patterns of the light mantle units in Av-10 create semi-circular patches on crater floors, crescent shapes around interior walls of craters, and irregular shapes that overlap crater rims and walls. The lobate pattern and well-defined edges of the light mantle patches are indicative of a fluid-like emplacement. There is almost no apparent relief associated with the deposits, indicating they are thin ( $\ll 1$  m?), surficial deposits. However, identifying source craters for light mantle deposits can be challenging. Geologic mapping of the light mantle (*lm*) units show how their distribution relates the other geologic units, local topography, and features within Av-10. Questions we investigate are, "What is the spatial relationship of the light mantle units to the other geologic mapping units?" and "Are some of the light mantle deposits distal ejecta from Oppia and Octavia?"

In Av-10, light mantle deposits are mapped within the boundaries of each of the major mapping units. The exposures of light mantle are loosely concentrated within four distinguishable zones within the quadrangle and are not evenly dispersed across the terrain. Going counterclockwise, these zones are (1) located northeast of Lepida crater, (2) along the eastern margin of the quadrangle in the cratered highlands terrain, (3) in the southeast quadrant along the Divalia Fossae Formation, and (4) around the western and northern rim of Oppia. The light mantle patches northeast of Lepida drape over both sharp rimmed and degraded craters. Despite the size of Lepida and proximity to these light mantle deposits,

no light mantle deposits are observed within its interior walls or along the outer rim and ejecta blanket. Lepida does not appear to be the source of the light mantle deposits in this area. Instead, craters north of Lepida in quadrangle Av-5 may be the source. In the northeast quadrant, within the cratered highlands terrain unit, the best example of light mantle crater rays in Av-10 are associated with an unnamed crater (10-km diameter, 358.20°E, 14.9°N). The light mantle rays are narrow and directed to the northwest and southeast up to 7 km from the rim. Patches in the southeastern quadrant have an east–west elongation and appear to drape along the troughs in the Divalia Fossae Formation. An unnamed crater (20 km diameter, 333°E, 12°S) ~100 km east of Oppia, has a distinctive patch of light mantle that overlaps the interior crater wall and extends 18 km to the northwest over the crater rim (Fig. 11g–i). The dark mantle on the western rim of Oppia is not as evenly distributed and appears disrupted by light mantle. It is difficult to tell if the light mantle was deposited before, after, or at the same time as the dark mantle and how much is related to the Oppia impact and the craters on the northwest rim. With respect to topography, the light mantle deposits are mapped within the higher topographic areas in Av-10 and are noticeably absent on the floor of Ferialia Planitia. Deposits that are mapped in lower elevations appear to be sourced from craters that formed at higher elevations. One idea presented in Le Corre et al. (2013) is that there is a near surface, discontinuous lithologic layer that when exposed by impact, results in the light mantle material. This unconfirmed unit layer could be ejecta material from Veneneia, Rheasilvia, or putative volcanic units that may have once covered parts of Vesta's surface. The lack of light mantle deposits associated with younger impact craters formed in topographically lower areas could support the idea that light mantle material is sourced from a near surface unit at higher elevations, though this layer may not be at a consistent elevation.

Determining the source craters for light mantle deposits can be difficult. Some light mantle deposits appear to have formed in association with a nearby crater. For example, the light mantle deposit shown in Fig. 11i (see also Fig. 3e and f in Le Corre et al., 2013) is widest at the crater rim and tapers downslope from the crater rim. There is also light mantle present on the interior crater wall. This particular deposit has several characteristics similar to lunar impact melt deposits including the flow-like appearance elongated in a downslope direction, deposition within 2 crater radii away from the rim, and its distribution direction coincides with the lowest part of the crater rim (Bray et al., 2010; Carter et al., 2012; Denevi et al., 2012; Neish et al., 2014; Le Corre et al., 2013). Light mantle deposits along the interior crater walls could represent a thin coating or veneer of impact melt as observed on lunar craters (Bray et al., 2010).

However, some patches of light mantle material do not have an obvious association with a nearby source crater. In these cases, we consider that the deposits could represent *distal ejecta*, impact material that has been deposited >5 crater radii away from the impact point (Glass and Simonson, 2012; Osinski and Pierazzo, 2013). Distal ejecta deposits are observed on Earth and the Moon, with deposits emplaced 100s to 1000s of kilometers away from the impact site (Addison et al., 2005; Schulte and Kontny, 2005; Schulte et al., 2009). Terrestrial distal ejecta deposits are centimeter to meter thick beds of glassy tektites and spherules (Addison et al., 2005; Glass and Simonson, 2012). Ejecta from Orientale basin has been emplaced up to 1000 km away from the impact center (Ghent et al., 2008). Light plains materials and smooth ponded features on the Moon were emplaced on nearly opposite sides of the lunar surface from the impact site (Robinson et al., 2010, 2011). On the Moon, for ponds with volumes >1 km<sup>3</sup>, a crater greater than >10 km diameter is required, but these ponds are not always found within the vicinity of craters of the necessary dimensions, with

crater age-models suggesting the deposits could come from a distal crater tens to hundreds of kilometers away (Robinson et al., 2011). While these deposits on the Moon are from large impact basins, not comparative in size to Oppia or Octavia on Vesta, we still must consider the possibility that these craters could produce distal ejecta deposits in low gravity environments. Distal ejecta are also more shocked than ejecta near the crater (Melosh, 1989). A basic equation for distance of ballistic trajectory of material is  $[d = (V^2 \sin 2\theta)/g]$  where  $d$  is distance,  $V$  is ejection velocity,  $\theta$  is ejection angle from horizontal surface, and  $g$  is the acceleration due to gravity of the planetary body. Gravity of Vesta is 0.25 m/s<sup>2</sup>, compared to gravity on the Moon is 1.622 m/s<sup>2</sup>, and Earth is 9.78 m/s<sup>2</sup>.

We propose that some of the light mantle deposits that do not appear to have a nearby source crater are distal ejecta deposits that have been transported from hundreds of kilometers away. Candidate source craters include Oppia and Octavia since they both have dark mantle continuous ejecta blankets and are geologically recent craters on the surface of Vesta (Williams et al., 2014; Schäfer et al., 2014). In Av-10, three different zones of light mantle can be mapped to the west, north, and northeast of Oppia (Fig. 13). The general patterns and elongation directions of some of the light mantle deposits in each zone are consistent with the respective transport directions from Oppia crater. The light mantle deposits are also at lower elevations and away from the lower elevation rim on Oppia, consistent with observations that lunar impact melt are commonly directed away from the lower portion of the crater rim (Neish et al., 2014). Light mantle deposits are up to ~300 km away from Oppia. As an example, for an ejection angle of 45°, material would need to have an ejection velocity ( $V$ ) of 168 m/s, 236 m/s, or 289 m/s to travel 100, 200, or 300 km respectively from the impact crater, not accounting for Vesta's spin rate (rotation rate: 5.342 h).

Light mantle deposits surrounding Octavia have characteristics that could also be consistent with distal ejecta. Light mantle deposits occur within a zone of ~300 km from the crater center (Fig. 14). One curious observation is that the majority of these light mantle deposits are consistently mapped on the interior crater walls that face toward Octavia (Fig. 14b and c) (Williams et al., 2014; Schäfer et al., 2014). For example, craters to the northwest of Octavia have crescent-shaped light mantle deposits on the interior walls that face southeast toward Octavia (Fig. 14b and d) (Williams et al., 2014; Schäfer et al., 2014). These craters have asymmetric topographic profiles with one wall of the crater higher than other. The light mantle deposits are mapped on the higher elevation walls, which face in the direction of Octavia. Similar observation can be made for craters to the southwest (Fig. 14c and e). One interpretation is that these light mantle deposits are veneers of impact melt that originated locally and are still preserved on the steeper slopes of these craters. An alternate interpretation is that they represent distal ejecta from Octavia that was deposited on the interior walls facing the direction of the ejecta. The material could have been on a transported ballistic trajectory or as a ground-hugging density flow similar to a base surge from a pyroclastic volcanic eruption (e.g., Carr et al., 1977; Melosh, 1989; Boyce et al., 2010). However, it is unclear if this style of emplacement of impact ejecta is likely on airless bodies without atmosphere to entrain the particles or how far the ejecta would travel across the surface in a low gravity environment and how the final morphology of the deposit would appear.

Light mantle deposits without clear nearby source craters could be distal ejecta deposits from larger craters such as Oppia and Octavia. We propose that the Oppia and Octavia impact events produced both the diffuse dark mantle deposited as continuous ejecta blanket and light mantle deposited as distal ejecta. The distribution of light mantle primarily on crater walls and scarps that face Octavia with no distinct deposits surrounding these craters could

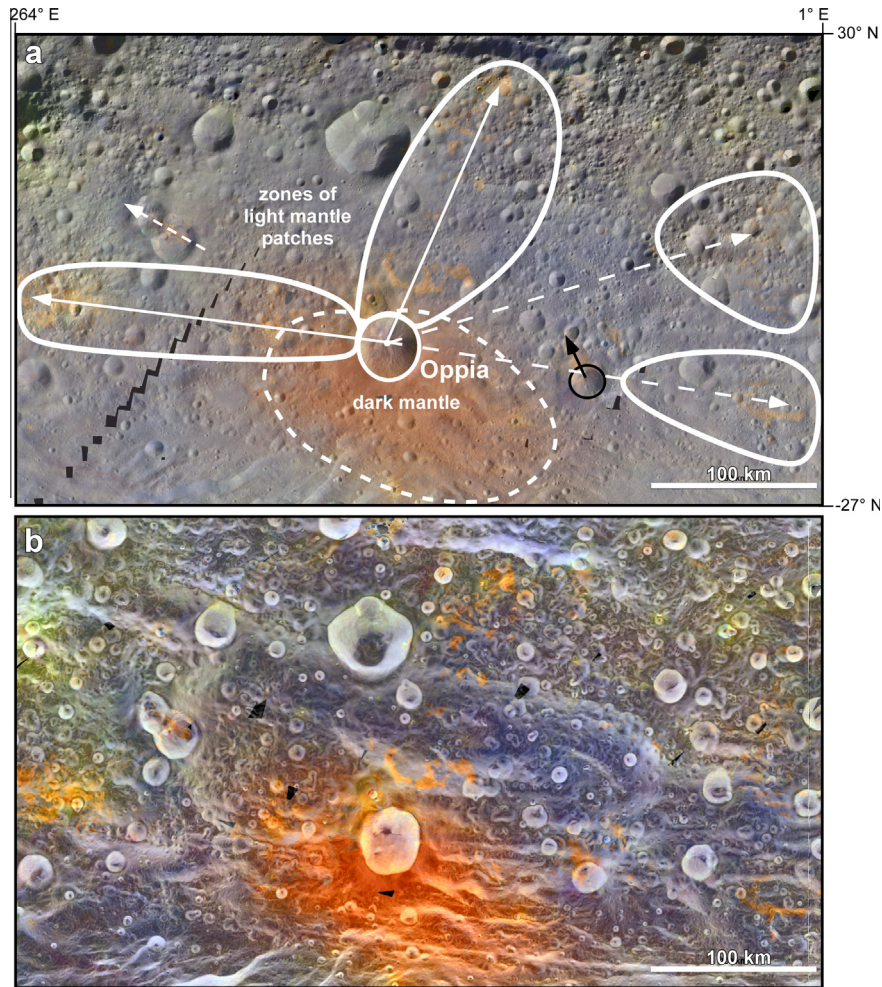


**Fig. 13.** Light mantle deposits in Av-10 mapped back toward Oppia crater. Arrows indicate transport direction (solid: ejecta from Oppia, dashed: possible ejecta direction). White circles mark crater rims with light mantle deposits. Black circle marks crater with light mantle deposit not associated with the Oppia impact. (b) Color-ratio overlay on slope map of Av-10. (For interpretation of the references to color in this figure legend, the reader is referred to the web version of this article.)

support the idea of distal ejecta in that we would expect to see additional light mantle deposits in the vicinity of these craters if it was produced locally, not just on the crater interior (Williams et al., 2014; Schäfer et al., 2014). Further studies on the dynamics of impact cratering processes on Vesta are warranted to understand how impact ejecta are distributed in microgravity environments (e.g., Melosh, 1989).

#### 4.2. Geologic history of Quadrangle Av-10: establishing a relative timescale for Vesta and small bodies

Geologic mapping of planetary bodies offers a unique challenge compared to traditional terrestrial field mapping (Sharp, 1988). The introductory paper for this issue provides an overview on the development of planetary mapping techniques for Vesta (Williams et al., 2014a). Here, we use Av-10 as a case study to introduce how geologic mapping can be used to define the relative stratigraphy and timescale for non-mappers.

The landscape contained within Av-10 provides a snapshot of Vesta's geologic history to discuss how these principles can be applied to planetary mapping. Features that have been discussed above form the framework of geologic events that we will discuss and place in a chronostratigraphic order. We first choose a prominent geologic feature to use as an arbitrary geologic benchmark and establish whether units are older or younger based on strati-

graphic principles. Here, we choose Feralia Planitia, because the size (5–15 km deep, 130 × 300 km), topography, and central location of this basin influences the landscape of Av-10. It is unclear if Feralia Planitia was created by multiple impact events, because its perimeter is modified by two trough systems and two prominent craters. First, we discuss the spatial relationships of the two trough systems to Feralia Planitia. The largest (widest) trough on Vesta, Saturnalia Fossa A, intersects Feralia Planitia in the northwest corner of Av-10. There is no topographic expression of the basin wall across the trough, which is to be expected if the trough formed after the basin and destroyed this section of the basin. Continuation of wall through the floor of Feralia Planitia is weakly apparent in topography and oblique images. The equatorial band of troughs and ridges that characterize Divalia Fossae Formation are present in the southeast quadrant of Av-10 and intersect the eastern wall of Feralia Planitia. Expressions of the ridge and trough system are also present on the floor of Feralia Planitia, but end at Oppia crater. The observation that the ridges and troughs have not been destroyed, suggests that the Divalia Fossae troughs are younger than Feralia Planitia. Both ridge and trough systems, Saturnalia Fossae Formation and Divalia Fossae Formation, are associated with the formation of two different south pole impact structures, Veneneia and Rheasilvia, respectively (Buczkowski et al., 2012; Schenk et al., 2012). Therefore, we can infer that the impact(s) that formed Feralia Planitia is/are older than the

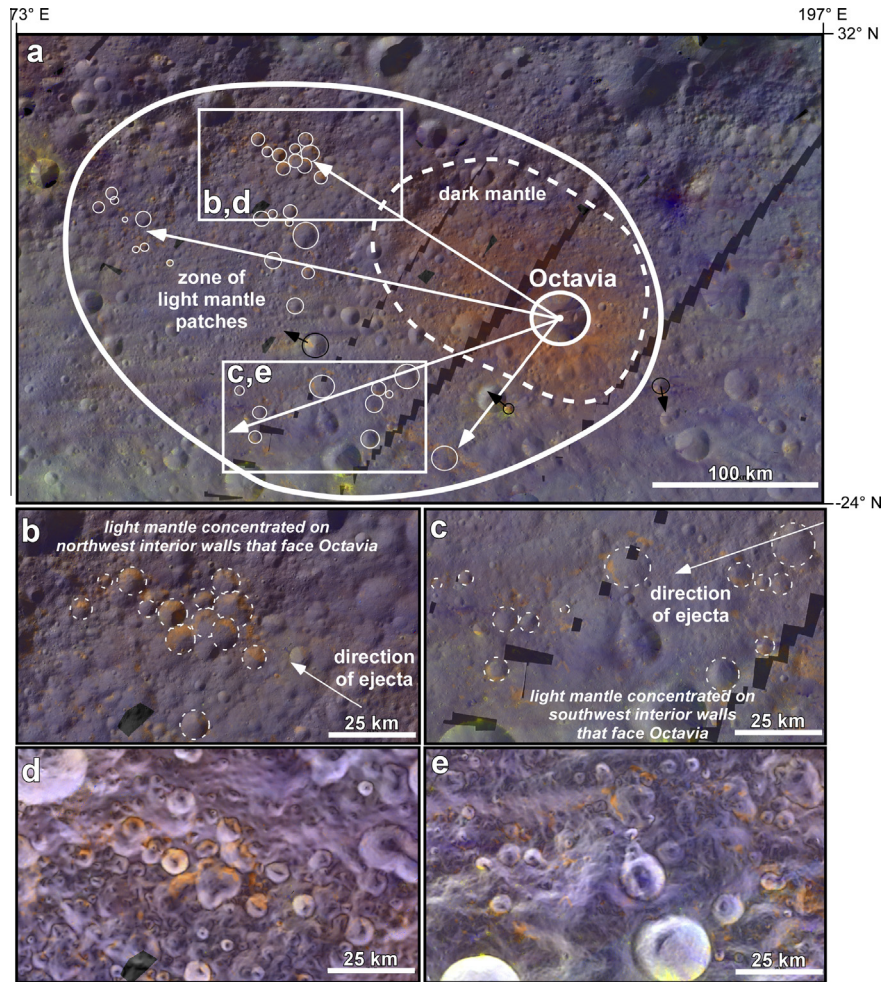


**Fig. 14.** Light mantle deposits mapped around Octavia crater ( $-24$  to  $32^{\circ}\text{N}$ ,  $73$ – $197^{\circ}\text{E}$ ). Arrows indicate transport direction. Extent of dark mantle and light mantle deposits surrounding the crater are outlined. (b) Craters northwest of Octavia, (c) craters southwest of Octavia, and slope maps with color ratio overlain for (d) northwest and (e) southwest craters. (For interpretation of the references to color in this figure legend, the reader is referred to the web version of this article.)

Veneneia and Rheasilvia impact events. The northern trough and equatorial trough systems do not intersect each other, therefore it is difficult to determine the relative age of these two trough systems based solely on observations of Av-10, without looking at the global mosaic or global geologic map (Yingst et al., 2014, in press).

Lepida ( $\sim 45$  km diameter) and Oppia ( $\sim 40$  km diameter) are two geologically young craters that formed on the northern and southern wall of Feralia Planitia, respectively. Lepida and Oppia both have sharp rims and relatively undisturbed ejecta blankets, so we infer that the impacts were relatively recent. Lepida also impacts along the transect of Saturnalia Fossa A and does not appear to be cut by the trough. Therefore we can infer that the Lepida impact occurred after the Veneneia impact. Oppia buries portions of the ridges and troughs in the Divalia Fossae Formation. The equatorial troughs of Divalia Fossae reach the eastern ejecta blanket of Oppia, but do not appear to cut through the main cavity. Looking at the slope map, ejecta from Oppia appears to divert around the ridges and between troughs, suggesting the troughs were present prior to the formation of the impact. If the troughs formed after the Oppia impact event, we would assume that the ejecta blanket and main crater wall would be cross-cut by the trough system. Instead, Oppia does not appear to have been influenced by any tectonic events. This would place the Divalia Fossae trough system as older than Oppia crater in the relative geologic timescale for Av-10. Tracing the edge of the Feralia Planitia basin in the topographic and slope maps shows that the basin wall

is also interrupted by Oppia. This indicates that Oppia is younger than both the Feralia and Rheasilvia impact events. Feralia Planitia is topographically low, and has been altered by structural troughs as well as two recent impact events, Lepida and Oppia. However, the cratered area in the northeast is topographically higher compared to Feralia Planitia and does not have any obvious troughs (maybe some subtle expression) cutting through the area. If we assume this area once continued across the basin, possibly connecting with Vestalia Terra (Av-9) (Buczkowski et al., 2014), then we can infer that the impact event(s) that created Feralia Planitia excavated the cratered highland material. Therefore, we place the highland material as the oldest material, followed by basin-forming impact events that excavated the basin in Feralia Planitia.

A basic geologic history of Av-10 can be recognized from the geologic map. The older cratered highlands represent some of the original, Pre-Veneneian crustal material on Vesta that was excavated by one or more impacts to form the basin Feralia Planitia. Both sets of troughs intersect the wall of Feralia Planitia indicating that this impact basin is older than both the Veneneia and Rheasilvia impact structures, thus also Pre-Veneneian in age. The northern trough and equatorial trough systems do not intersect each other, therefore it is difficult to determine which system is older based on the field of view of Av-10, without looking at the global geologic map (Yingst et al., 2014, in press). The relatively youngest units in Av-10 are several geologically young craters that have formed in the aforementioned terrains and geologic structures, resurfacing

portions of them with ejecta. A rudimentary timescale can be created based on the units and events mapped in Av-10. The oldest time period would be defined by the ancient terrains and impacts that occurred early on in the formation of Vesta. The northern and equatorial trough systems are global features associated with two major impact basins that each define distinct geologic moments in the history of Vesta and two younger periods of time. The younger periods of geologic time in Av-10 can be defined by events that occurred after the formation of Rheasilvia basin and defined Oppia impact crater. The geologic map of Av-10 provides examples of several key geologic features on the asteroid and serves as a snapshot of the relative geologic history of Vesta.

A preliminary time-stratigraphic system for Vesta is proposed based on major rock units and events defined through the global geologic mapping (Williams et al., 2014b). Four time units are defined based on various rock units: *Pre-Veneneian Period*, *Veneneian Period*, *Rheasilvian Period*, *Marcian Period*. The block of time that each period encompasses varies based on which chronology function is used to define the vestan chronology system (lunar-derived or asteroid-derived) (e.g., O'Brien et al., 2014; Schmedemann et al., 2014). Time-stratigraphic systems for asteroids are not common, but Vesta is large enough in size and has enough distinctive features and rock units preserved that one can be established. From our mapping, it is clear that all four vestan time-stratigraphic systems and time periods occur in this quadrangle: cratered highlands and cratered plains of Feralia Planitia are Pre-Veneneian; Saturnalia Fossae Formation is Veneneian; Divalia Fossae Formation and Rheasilvia Formation are Rheasilvian; and some of the younger crater material (e.g., Paulina) are probably Marcian.

## 5. Conclusions

Geologic mapping of Oppia Quadrangle Av-10 (288–360°E, ±22°) shows that this area is a junction of key geologic features that preserve a rough geologic history of Asteroid (4) Vesta and is a contained case study to define a relative geologic timescale for Vesta. Quadrangle Av-10 contains geologic map units that are representative of each of the vestan time-stratigraphic systems and time periods: cratered highlands terrain, cratered plains material, Saturnalia Fossae Formation trough terrain, Divalia Fossae Formation trough terrain, crater wall and ejecta, dark crater rays, and light and dark mantle. The cratered highlands terrain is the oldest unit in Av-10 and represents crustal material on Vesta that was excavated to form the basin Feralia Planitia and the cratered plains unit, both of which are Pre-Veneneian in age. The two terrains characterized by ridge and trough systems, Saturnalia Fossae Formation trough terrain and Divalia Fossae Formation trough terrain, are Veneneian and Rheasilvian in age, respectively. The relatively youngest geologic units/features in Av-10 are several relatively young craters that have formed in the aforementioned terrains and are either Late Rheasilvian in age or Marcian (e.g., Lepida, Oppia, Paulina craters). Mapping of the light mantle and dark mantle units in Av-10 supports previous interpretations of impact ejecta (impact melt) origin. Observations suggest that some light mantle deposits could be distal ejecta from Oppia and Octavia, deposited 100s of km away from the craters.

## Acknowledgments

The authors would like to thank the Dawn flight, operations, and science teams at Jet Propulsion Laboratories, the instrument teams at the German Aerospace Center (DLR), the Italian National Institute for Astrophysics (INAF), Max Planck Institute, and the Planetary Science Institute. Thank you to Dr. J. Olaf Gustafson, an anonymous reviewer, and Guest Editor, Dr. David Blewett, for their thorough

comments, edits, and suggestions. Support for W.B. Garry's research and writing of this manuscript was funded by the Dawn at Vesta Participating Scientist Program Grants NNX10AR28G (Smithsonian), NNX11AK16G (Planetary Science Institute), and award to NASA Goddard Space Flight Center. The data used in this paper are available from the website <http://dawndata.igpp.ucla.edu>.

## Appendix A. Supplementary material

Supplementary data associated with this article can be found, in the online version, at <http://dx.doi.org/10.1016/j.icarus.2014.08.046>.

## References

- Addison, W.D. et al., 2005. Discovery of distal ejecta from the 1850 Ma Sudbury impact event. *Geology* 33 (3), 193–196.
- Ammannito, E. et al., 2013. Olivine in an unexpected location on Vesta's surface. *Nature* 504, 122–125.
- Boyce, J. et al., 2010. Rampart craters on Ganymede: Their implications for fluidized ejecta emplacement. *Meteoritics and Planetary Science* 45 (4), 638–661.
- Bray, V.J. et al., 2010. New insight into lunar impact melt mobility from the LRO camera. *Geophys. Res. Lett.* 37 (21), L21202. <http://dx.doi.org/10.1029/2010GL044666>.
- Buczkowski, D.L. et al., 2012. Large-scale troughs on Vesta: A signature of planetary tectonics. *Geophys. Res. Lett.* 39, L18205.
- Buczkowski, D.L. et al., 2014. The unique geomorphology and physical properties of the Vestalia Terra plateau. *Icarus* 244, 89–103.
- Carr, M.H., Crumpler, L.S., Cutts, J.A., Greeley, R., Guest, J.E., Masursky, H., 1977. Martian impact craters and emplacement of ejecta by surface flow. *J. Geophys. Res.* 82 (28), 4055–4065.
- Carter, L.M. et al., 2012. Initial observations of lunar impact melts and ejecta flows with the Mini-RF radar. *J. Geophys. Res.* 117, E00H09. <http://dx.doi.org/10.1029/2011JE003911>.
- Christensen, P.R. et al., 2009. JMARS—A planetary GIS. American Geophysical Union (Fall). Abstracts (vol. 1, p. 06). <<http://adsabs.harvard.edu/abs/2009AGUFMIN22A.06C>>.
- De Sanctis, M.C. et al., 2011. The VIR spectrometer. *Space Sci. Rev.* 163, 329–369.
- De Sanctis, M.C. et al., 2012. Spectroscopic characterization of mineralogy and its diversity across Vesta. *Science* 336 (6082), 697–700. <http://dx.doi.org/10.1126/science.1219270>.
- De Sanctis, M.C. et al., 2014. Compositional evidence of magmatic activity on Vesta. *Geophys. Res. Lett.* 41, 3038–3044.
- Denevi, B.W., Koeber, S.D., Robinson, M.S., Garry, W.B., Hawke, B., Tran, T.N., Tornabene, L.L., 2012. Physical constraints on impact melt properties from Lunar Reconnaissance Orbiter Camera images. *Icarus* 219 (2), 665–675.
- Gaskell, R.W., 2012. SPC shape and topography of Vesta from DAWN Imaging Data. In: AAS/Division for Planetary Sciences Meeting Abstracts 44, Abstract #209.03.
- Ghent, R.R., Campbell, B.A., Hawke, B.R., Campbell, D.B., 2008. Earth-based radar data reveal extended deposits of the Moon's Orientale basin. *Geology* 36 (5), 343–346.
- Glass, B.P., Simonson, B.M., 2012. Distal impact ejecta layers: Spherules and more. *Elements* 8 (1), 43–48.
- Jaumann, R. et al., 2012. Vesta's shape and morphology. *Science* 336, 687–690.
- Kneissl, T. et al., 2014. Morphology and Formation Ages of mid-sized post-Rheasilvia craters – Geology of quadrangle Tuccia, Vesta. *Icarus* 244, 133–157.
- Krohn, K. et al., 2013. Asymmetric Craters on Vesta: Formation on Sloping Surfaces. EPSC, Abstract #EPSC2013-488.
- Le Corre, L., Reddy, V., Nathues, A., Cloutis, E.A., 2011. How to characterize terrains on 4 Vesta using Dawn Framing Camera color bands? *Icarus* 208, 238–251.
- Le Corre, L. et al., 2013. Olivine or impact melt: Nature of the “Orange” material on Vesta from Dawn. *Icarus* 226, 1568–1594.
- Marchi, S. et al., 2012. The violent collisional history of Asteroid 4 Vesta. *Science* 336, 690–694.
- Marchi, S. et al., 2014. Small crater populations on Vesta. *Planet. Space Sci.* (in press), <http://dx.doi.org/10.1016/j.pss.2013.05.005>.
- McCord, T.B., Adams, J.B., Johnson, T.V., 1970. Asteroid Vesta: Spectral reflectivity and compositional implications. *Science* 168, 1445–1447.
- McSween, H.Y. et al., 2013. Dawn; the Vesta–HED connection; and the geologic context for eucrites, diogenites, and howardites. *Meteorit. Planet. Sci.* 48, 2090–2104.
- Melosh, H.J., 1989. *Impact Cratering: A Geologic Process*. Research Supported by NASA. Oxford University Press, New York, 253p., 1 (Oxford Monographs on Geology and Geophysics, No. 11).
- Neish, C.D. et al. (2014, March). Global distribution of lunar impact melt flows. *Lunar Planet. Sci.* 45, 1159 (Abstracts).
- O'Brien, D.P. et al., 2014. Constraining the cratering chronology of Vesta. *Planet. Space Sci.* <http://dx.doi.org/10.1016/j.pss.2014.05.013>.
- Osinski, G.R., Pierazzo, E., 2013. *Impact Cratering: Processes and Products*. John Wiley & Sons.

- Pieters, C.M., Staid, M.I., Fischer, E.M., Tompkins, S., He, G., 1994. A sharper view of impact craters from Clementine data. *Science* 266, 1844–1848.
- Pope, Kevin O. et al., 2005. Chicxulub Impact Ejecta Deposits in Southern Quintana Roo, México, and Central Belize. Geological Society of America Special Papers 384, pp. 171–190.
- Prettyman, T.H. et al., 2011. Dawn's gamma ray and neutron detector. *Space Sci. Rev.* 163, 371–459.
- Prettyman, T.H. et al., 2012. Elemental mapping by Dawn reveals exogenic H in Vesta's howarditic regolith. *Science* 338, 242–246.
- Rayman, M.D., Fraschetti, T.C., Raymond, C.A., Russell, C.T., 2006. Dawn: A mission in development for exploration of main belt asteroids Vesta and Ceres. *Acta Astronaut.* 58, 605–616.
- Reddy, V. et al., 2012. Albedo and color heterogeneity of Vesta from Dawn. *Science* 336, 700–704.
- Roatsch, T. et al., 2012. High resolution Vesta High Altitude Mapping Orbit (HAMO) atlas derived from Dawn Framing Camera images. *Planet. Space Sci.* 73, 283–286.
- Robinson, M.S. et al., 2010. Impact melts on the Moon: How far will they go? American Geophysical Union (Fall). Abstracts 1, 02.
- Robinson, M.S. et al., 2011. Highland smooth plains, an exceptional grouping. *Lunar Planet. Sci.* 42, 2511 (Abstracts).
- Ruesch, O., et al., 2014. Geologic map of the northern hemisphere of Vesta based on Dawn Framing Camera (FC) images. *Icarus* 244, 41–49.
- Russell, C.T., Raymond, C.A., 2011. The Dawn mission to Vesta and Ceres. *Space Sci. Rev.* 163, 3–23.
- Russell, C.T. et al., 2004. Dawn: A journey in space and time. *Planet. Space Sci.* 52, 465–489.
- Russell, C.T. et al., 2012. Dawn at Vesta: Testing the protoplanetary paradigm. *Science* 336, 684–686.
- Schäfer, M. et al., 2014. Imprint of the Rheasilvia impact on Vesta – Geologic mapping of quadrangles Gegania and Lucaria. *Icarus* 244, 60–73.
- Schenk, P. et al., 2012. The geologically recent giant impact basins at Vesta's south pole. *Science* 336, 694–697.
- Schmedemann, N. et al., 2014. The cratering record, chronology and surface ages of (4) Vesta in comparison to smaller asteroids and the ages of HED meteorites. *Planet. Space Sci.* <http://dx.doi.org/10.1016/j.pss.2014.04.004>.
- Schulte, P., Kontny, A., 2005. Chicxulub Impact Ejecta from the Cretaceous–Paleogene (KP) Boundary in Northeastern México. Geological Society of America Special Papers 384, pp. 191–221.
- Schulte, P. et al., 2009. A dual-layer Chicxulub ejecta sequence with shocked carbonates from the Cretaceous–Paleogene (K–Pg) boundary, Demerara Rise, western Atlantic. *Geochim. Cosmochim. Acta* 73 (4), 1180–1204.
- Scully, J.E.C. et al., 2014. Geomorphology and structural geology of Saturnalia Fossae and adjacent structures in the northern hemisphere of Vesta. *Icarus* 244, 23–40.
- Sharp, R.P., 1988. Earth science field work: Role and status. *Ann. Rev. Earth Planet. Sci.* 16, 1–19.
- Sierks, H. et al., 2011. The Dawn Framing Camera. *Space Sci. Rev.* 163, 263–327.
- Tosi, F. et al., 2014. Thermal measurements of dark and bright surface features on Vesta as derived from Dawn/VIR. *Icarus* 240, 36–57. <http://dx.doi.org/10.1016/j.icarus.2014.03.017>.
- Wilhelms, D.E., 1990. Geologic mapping. In: Greeley, R., Batson, R.M. (Eds.), *Planetary Mapping*. Cambridge University Press, New York, pp. 208–260.
- Williams, D.A., et al., 2014. The Geology of the Marcia Quadrangle of Asteroid Vesta: Assessing the effects of large, young, craters. *Icarus* 244, 74–88.
- Williams, D.A., Yingst, R.A., Garry, W.B., 2014a. Introduction: The geologic mapping of Vesta. *Icarus* 244, 1–12.
- Williams, D.A., et al., 2014b. Proposed time-stratigraphic system of Vesta. *Icarus* 244, 158–165.